LANGMUIR

pubs.acs.org/Langmuir Article

New Insights into Spin Coating of Polymer Thin Films in Both Wetting and Nonwetting Regimes

Yuxin Jiang, Margaret Minett, Elizabeth Hazen, Wenyun Wang, Carolina Alvarez, Julia Griffin, Nancy Jiang, and Wei Chen*

Cite This: https://doi.org/10.1021/acs.langmuir.2c02206 Read Online

ACCESS | Metrics & More | Article Recommendations | Supporting Information

ABSTRACT: Spin coating is a common method for fabricating polymer thin films on flat substrates. The well-established Meyerhofer relationship between film thickness (h) and spin rate (ω), $h \propto \omega^{-1/2}$, enables the preparation of thin films with desired thickness by adjusting the spin rate and other experimental parameters. The 1/2 exponent has been verified by previous studies involving organic thin films prepared on silicon wafers. In this study, 88% and >99% hydrolyzed poly(vinyl alcohol) (PVOH) polymers were adsorbed and spin-coated from an aqueous solution onto four different substrates. The substrates were prepared by covalently attaching poly(dimethylsiloxane) (PDMS) of different molecular weights onto silicon wafers (SiO_2). Atomic force microscopy images indicate that the PVOH films transitioned from stable on SiO_2, to metastable, and then to unstable as PDMS molecular weight was increased. Notably, none of the polymer−substrate systems studied here exhibited the thickness-spin rate profile predicted by the Meyerhofer model. Based on the experimental results, a more general adsorption−deposition model is proposed that decouples the total spin-coated thickness into two components—the adsorbed thickness (h_1) and the spin-deposited thickness (h_2). The former accounts for polymer−substrate interactions, and the latter depends on polymer concentration and spin rate. In unstable systems, the exponents were found to be ∼0 because slip takes place at the solution−substrate interface during spin and the spin-deposited thickness is 0. In metastable and stable systems, a universal relationship between spin-deposited thickness and spin rate emerged, independent of the substrate type and polymer concentration for each polymer examined. Our findings indicate the importance of film stability and polymer−substrate interactions in the application of spin coating.

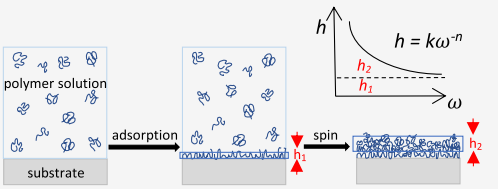

INTRODUCTION

The stability of polymer thin films has been studied extensively[1−8] because of its relevance in science, technology, and everyday life. While stable, pinhole-free thin films are often desirable, controlled dewetting has become increasingly important in many arenas, such as lithography, nanoscience, and biotechnology. Some excellent reviews have summarized dewetting theories and advances in applying dewetting toward the generation of ordered surface patterns.[9−12] The effective interface potential, $\phi(h)$, is defined as the excess free energy per unit area necessary to bring solid−liquid and liquid−gas interfaces from infinity to thickness h. Figure 1 depicts the three scenarios—stable (curve 1), unstable (curve 2), and metastable (curve 3) systems.[8] A polymer−substrate system is considered stable when $\phi(h) > 0$ is met in the entire thickness range. A system is considered unstable when there is a global minimum. A metastable system has the combined features of the unstable (at low film thicknesses) and stable (at large film thicknesses) curves. When $\phi''(h) < 0$ is met in unstable and metastable systems, spinodal dewetting, caused by amplified capillary waves, takes place to produce holes separated by a characteristic wavelength. Around $\phi''(h) = 0$ beyond the local maximum in metastable systems, thermal or homogeneous nucleation can occur to produce randomly distributed holes of

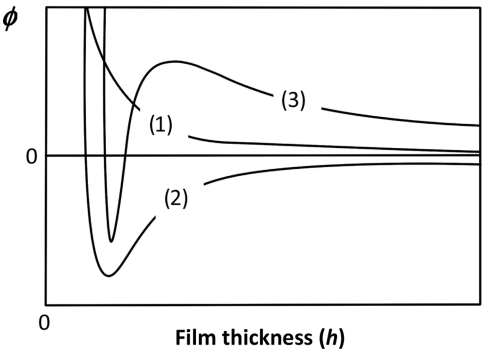

Figure 1. Effective interface potential, ϕ, as a function of film thickness (h) for stable (curve 1), unstable (curve 2), and metastable (curve 3) films.

Received: August 15, 2022
Revised: September 21, 2022

different sizes. Another mechanism of dewetting is heterogeneous nucleation, which is caused by surface defects and generates holes of similar sizes.[8] The initially generated holes can grow, merge, and rupture, resulting in honeycombs, ribbons, and/or droplets due to Rayleigh instabilities.[2]

Most of the systems studied thus far involved nonpolar, nonvolatile van der Waals thin films on nonwetting solids, such as polystyrene films on silicon wafers. The fundamental, environmental, and technological significance of hydrophilic polymer thin films prepared from an aqueous solution necessitates a robust understanding of their stability.[4] The destabilizing polar interactions during solvent evaporation, however, present additional challenges in the studies of these thin films.[6] Thiele et al. studied the stability of collagen thin films spin-coated from an aqueous solution on highly oriented pyrolytic graphite.[6] Heterogeneous nucleation in thick films and spinodal decomposition caused by destabilizing polar interactions in thinner films were observed. In another study, fibronectin (FN) was adsorbed to poly(alkyl acrylate) substrates from an aqueous solution.[13] It was found that the extent of FN dewetting increased as the alkyl chain length increased. A related simulation study revealed that the disruption of the hydration layer by the longer and more mobile alkyl segment facilitated FN fibrillogenesis.[14]

Among the methods for polymer thin-film preparation, spin coating is widely used because of its low cost and reproducibility.[15,16] It consists of deposition, spin-up, spin-off, and solvent evaporation steps.[17] One of the shortcomings of the conventional spin-coating method is the variable amount of time between deposition and spin-up, which can cause irreproducibility in situations where polymer spontaneously adsorbs at the solution−substrate interface. We recently addressed this issue and introduced the "adsorptive spin-coating" method, which includes a deliberate adsorption step between the deposition and spin-up steps.[18,19]

Being able to predict and control film thickness is an important consideration in choosing the spin-coating technique. For a nonvolatile, Newtonian solution on a rotating disk, the balance between centrifugal and viscous forces results in films of uniform thickness, assuming no slip at the solution−substrate interface.[20] Meyerhofer proposed a model to decouple outward flow and evaporation, allowing the prediction of film thickness (h) as a function of spin rate (ω), $h = k\omega^{-1/2}$, where k is related to the initial solution viscosity.[21] The model does not account for polymer−substrate and polymer−polymer interactions. Despite the simplicity of the model, it has had tremendous success at fitting experimental data, e.g., Extrand and Danglad-Flores confirmed the 1/2 exponent for different organic polymers spin-coated on silicon wafers.[22−24] Deviations from the Meyerhofer prediction have also been reported. An exponent greater than 1/2 is attributed to inadequate spin time at low spin rates, shear thinning at high spin rates,[25,26] and/or polymer concentrations higher than 2 wt %.[24] On the other hand, an exponent lower than 1/2 is due to the effect of fluid inertia at high spin rates.[25]

The spontaneous adsorption of poly(vinyl alcohol) (PVOH) to hydrophobic substrates was reported two decades ago.[27−31] The substrates investigated include fluoropolymers,[27−29] polyolefins,[27−29] polyesters,[27−29] polystyrene,[30] and gold.[31] PVOH is atactic yet semi-crystalline. The driving forces for the adsorption include hydrophobic interactions and the subsequent crystallization of PVOH polymer chains at the solid−solution interface.[28] Kinetics studies indicated that PVOH adsorption is fast, within minutes.[27,28] The adsorbed PVOH thin films appeared continuous by atomic force microscopy (AFM) with reproducible thicknesses.[28,29] Recently, we evaluated adsorption and adsorptive spin coating of PVOH on poly(dimethylsiloxane) (PDMS) substrates.[18,32] The PVOH thin films underwent more extensive dewetting as PDMS molecular weight (thickness) was increased. The film instability was attributed to substrate mobility. Stepwise dewetting dynamics of PVOH drops were captured using high-speed photography.[18]

In this study, PVOH thin films were fabricated on SiO_2-PDMS composite substrates using the adsorptive spin-coating method. Stable, metastable, and unstable systems were attained by adjusting substrate energetics and mobility. A new model is proposed to elucidate the relationship between spin-coated thickness and spin rate in all three systems.

EXPERIMENTAL SECTION

Materials. Silicon wafers (100 orientation, P/B doped, resistivity 1−10 Ω·cm, thickness 475−575 μm) were purchased from International Wafer Service. Poly(vinyl alcohol) polymers ($PVOH^{99\%H}$: MW = 89−98 kDa, >99% hydrolyzed, batch #06521TH; $PVOH^{88\%H}$: MW = 85−124 kDa, 88% hydrolyzed, batch #09501BE) were obtained from Sigma-Aldrich. Trimethylsilyl-terminated poly(dimethylsiloxanes) (PDMS) ranging from 237 Da to 116 kDa in molecular weight were purchased from Gelest. HPLC-grade organic solvents were obtained from Pharmco. Oxygen gas (99.999%) was purchased from Airgas. Nitrogen gas (99.998%) was purchased from Ivey Industries. All reagents were used as received without further purification. Water was purified using a Millipore Milli-Q Biocel System (Millipore Corp., resistivity ≥18.2 MΩ/cm). Glassware was cleaned in a base bath (potassium hydroxide in isopropyl alcohol and water), rinsed with deionized water, and stored in an oven at 110 °C until use.

Instrumentation and Characterization. Silicon wafers were cleaned in a Harrick plasma cleaner PDC-001. Spin coating was carried out using a Laurell WS-650MZ-23NPPB spin coater. Dynamic light scattering (DLS) measurements were carried out using a Malvern Zetasizer Nano-S equipped with a 4 mW He−Ne laser (λ = 632.8 nm) to determine the size of PVOH chains in solution. Refractive indices of PVOH (n = 1.520) and water (n = 1.330) and viscosity of water (η = 0.8872) at 25 °C were assigned. Contact angles were measured using a Ramé-Hart telescopic goniometer with a Gilmont syringe and a 24-gauge flat-tipped needle. Dynamic advancing and receding angles were captured by a camera and digitally analyzed while Milli-Q water in the syringe was added to and withdrawn from the drop, respectively. The standard deviation of the reported contact angle values is less than or equal to 2° unless specified otherwise. Native silicon dioxide and polymer layer thicknesses were measured using a Gaertner Scientific LSE Stokes ellipsometer at a 70° incident angle (from the normal to the plane). The light source is a He−Ne laser (λ = 632.8 nm). Thickness was calculated using the following refractive indices: air, n_o = 1; silicon oxide and polymer layers, n_1 = 1.46; silicon substrate, n_s = 3.85, and k_s = −0.02 (absorption coefficient). Measurement error is within 1 Å, as specified by the manufacturer. Each reported thickness and contact angle value is an average of at least eight measurements obtained from at least four samples from two different batches and two readings from different locations on each sample. Nanoscopic surface topography was imaged using a Veeco Metrology Dimension 3100 atomic force microscope (AFM) with a silicon tip operating in tapping mode. Roughness and section analyses of surface features were determined using Nanoscope software. Multiple AFM images from different samples of the same type and different locations on each sample were captured; representative images were chosen.

Preparation of Substrates. Silicon wafers were diced into 1.4 cm × 1.4 cm pieces, rinsed with deionized water, and dried with

https://doi.org/10.1021/acs.langmuir.2c02206
Langmuir XXXX, XXX, XXX−XXX

Table 1. Thickness (T), Advancing, Receding, and Average Water Contact Angles ($\theta_{Ad}/\theta_{Re}/\theta_{Avg}$) and Surface Fractions of PDMS (f_2) on PDMS Substrates with Different Molecular Weights

	PDMS^{237}	PDMS^{340}	PDMS^{550}	PDMS^{770}	PDMS^{2k}	PDMS^{9k}	PDMS^{17k}	PDMS^{49k}	PDMS^{116k}
T (nm)	0.27 ± 0.1	0.18 ± 0.1	0.76 ± 0.1	0.82 ± 0.1	1.2 ± 0.2	3.6 ± 0.4	4.4 ± 0.4	7.6 ± 0.5	11.3 ± 0.7
θ_{Ad} (deg)	60 ± 3	58 ± 4	103 ± 2	102 ± 2	101 ± 2	107 ± 2	109 ± 2	109 ± 2	113 ± 2
θ_{Re} (deg)	26 ± 4	22 ± 6	84 ± 2	78 ± 3	79 ± 3	102 ± 2	104 ± 2	95 ± 2	98 ± 2
θ_{Avg} (deg)	43 ± 3	40 ± 4	93.5 ± 2	90 ± 2	90 ± 2	104.5 ± 2	106.5 ± 2	102 ± 2	105.5 ± 2
f_2	~0.3 (LMW)		~0.9 (MMW)			~1 (HMW)			

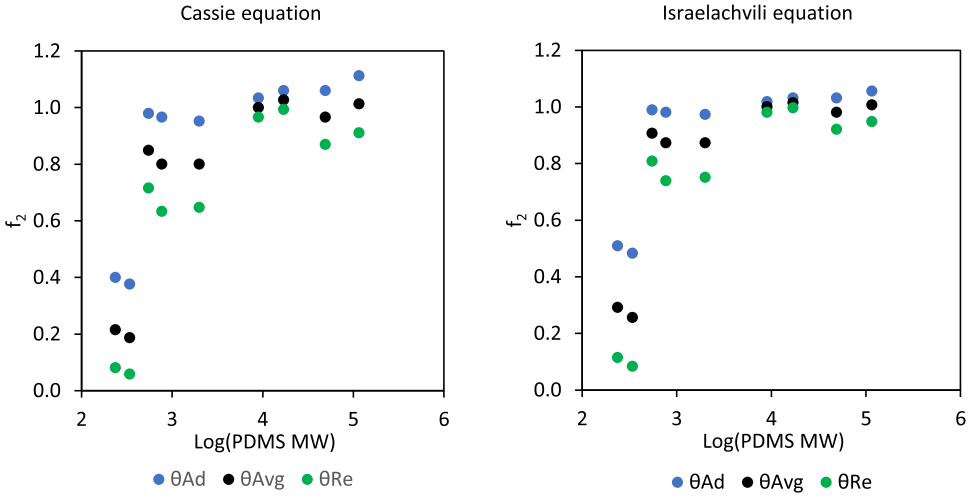

Figure 2. Surface fraction of PDMS, f_2, as a function of PDMS molecular weight using the Cassie (left) and Israelachvili (right) equations.

compressed air in a clean oven at 110 °C for 30 min prior to being exposed to oxygen plasma at ~300 mTorr and 30 W for 15 min. The freshly prepared silicon wafers (SiO_2) were immediately used for PVOH deposition or reacting with PDMS polymers to prepare SiO_2/PDMS substrates. In the latter case, 100 μL of PDMS polymer was dispensed on each clean wafer. The samples were heated at 100 °C for 24 h in capped scintillation vials. After the reaction, the samples were rinsed individually with toluene (3×), ethanol (3×), and Milli-Q water (3×), dried under a nitrogen stream to remove excess water, and stored in a desiccator ($CaSO_4$) overnight.

Preparation of PVOH Solutions. PVOH solutions of various concentrations, from 0.05 to 0.5 wt %, were prepared by dissolving desired amounts of PVOH powder in 100 g of Milli-Q water at 88−94 °C for 3 h under stirring in clean poly(propylene) bottles. After equilibration for a few days, the PVOH solutions were characterized using DLS to ensure complete polymer dissolution. The solutions were used within 90 days of preparation.

Static Adsorption of PVOH. A drop of PVOH solution of a desired volume (100 μL on SiO_2 and 400 μL on SiO_2/PDMS) was dispensed onto a substrate. After 1 min, the sample was rinsed with Milli-Q water (3×), dried under a nitrogen stream, and stored in a desiccator ($CaSO_4$) overnight.

Adsorptive Spin Coating of PVOH. A drop of PVOH solution of a desired volume (100 μL on SiO_2 and 400 μL on SiO_2/PDMS) was dispensed onto a substrate secured on the spin coater stage. After 1 min, the sample was spun at a desired rate (900−6000 rpm) for 1 min under nitrogen. The sample was stored in a desiccator ($CaSO_4$) overnight prior to characterization.

Thermal Annealing. Supported PVOH thin films were heated at 100 °C for a desired amount of time in capped scintillation vials. They were characterized immediately after cooling to room temperature.

RESULTS AND DISCUSSION

Four Types of Substrates. PDMS polymers of different molecular weights (MW) were covalently attached to silicon wafers to prepare substrates with varying surface composition, hydrophobicity, and mobility. As the PDMS molecular weight increases from 237 Da to 116 kDa, the PDMS layer thickness as well as water contact angles increase as a result of increased surface coverage of PDMS on silicon wafers, as shown in Table 1. These trends are consistent with an earlier publication.[33] Based on the AFM images, the PDMS substrates are featureless up to PDMS^{2k} and become noticeably rougher as the PDMS molecular weight increases.[33]

The substrates were treated as binary composites consisting of f_1 surface fraction of component 1 (SiO_2) and f_2 surface fraction of component 2 (PDMS), with $f_1 + f_2 = 1$. The Cassie equation[34] (eq 1) and the Israelachvili equation[35] (eq 2) allow the determination of surface composition of a composite based on the contact angle values of the composite (θ), pure component 1 (θ_1), and pure component 2 (θ_2). The Cassie equation is more suitable for surfaces with well separated and distinct patches, while the Israelachvili equation works better for surfaces with molecular-level chemical heterogeneities.[35]

$$\cos\theta = f_1 \cos\theta_1 + f_2 \cos\theta_2 \quad (1)$$

$$(1 + \cos\theta)^2 = f_1(1 + \cos\theta_1)^2 + f_2(1 + \cos\theta_2)^2 \quad (2)$$

It is reasonable to assume $\theta_1 = 0$ since water completely spreads on a clean silicon wafer. As PDMS molecular weight increases, more silicon wafer surface is covered by PDMS. Further increasing PDMS molecular weight beyond complete surface coverage results in larger surface roughness and increased contact angle hysteresis (larger advancing and lower receding contact angles).[32] This is illustrated in Table 1—both PDMS^{49k} and PDMS^{116k} exhibit higher contact angle hysteresis than PDMS^{9k} and PDMS.^{17k} Thus, the average of the advancing (107°) and receding (102°) contact angles on PDMS^{9k} is used for θ_2, 104.5°. For θ values, advancing contact angle (θ_{Ad}), receding contact angle (θ_{Re}), and the average of

https://doi.org/10.1021/acs.langmuir.2c02206
Langmuir XXXX, XXX, XXX−XXX

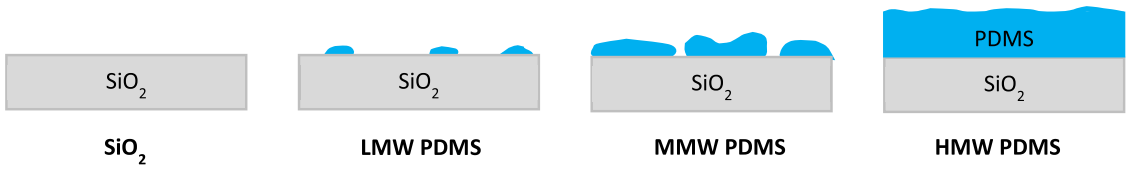

Figure 3. Four types of substrates with varying surface compositions.

Table 2. AFM Images (Size: 1.25 μm × 5 μm; Height Scale: 5 nm) of PVOH$^{99\%H,0.1wt\%}$ Thin Films Fabricated on SiO_2, PDMS^{340}, and PDMS^{2k} Substrates at Spin Rates from 900 rpm (Thickest) to 6000 rpm (Thinnest)

Spin rate (rpm)	SiO_2	PDMS^{340}	PDMS^{2k}
900			
1400			
2200			
3500			
4800			
6000			

the two angles (θ_{Avg}) were used respectively to calculate surface compositions. Figure 2 depicts surface fraction of PDMS, f_2, as a function of PDMS molecular weight using the Cassie and Israelachvili equations.

Some observations and comments can be made based on Figure 2. (1) At high PDMS coverage (PDMS^{9k} to PDMS^{116k}), the two equations predict similar surface compositions, while at low and intermediate coverage, the Israelachvili equation predicts higher f_2 values. (2) Considering that the low to intermediate molecular weight PDMS polymers (PDMS^{237} to PDMS^{2k}) are molecular in dimension and too small to be considered "patches," the Israelachvili equation is a more suitable model to predict surface compositions. (3) Surfaces containing low and high molecular weights of PDMS have high contact angle hysteresis due to chemical heterogeneity and surface roughness, respectively. Thus, using the average of advancing and receding contact angles should minimize these effects. It is worth noting that both equations require the use of thermodynamic contact angles, which fall between advancing and receding contact angles. In this study, average contact angles are used as estimates and should not be construed as thermodynamic contact angles. (4) Even using the average contact angle values results in $f_2 > 1$ when PDMS molecular weights are very high. In such cases, f_2 is considered to be 1. Therefore, the Israelachvili equation and the average water contact angles allow us to predict the PDMS surface coverage on the various substrates used in this research: f_2 = ~0.3 on low MW (LMW) PDMS (237 and 340), f_2 = ~0.9 on intermediate MW (MMW) PDMS (550, 770, and 2k), and f_2 = ~1 on high MW (HMW) PDMS (9k, 17k, 49k, and 116k). This result is summarized in the last row of Table 1. The four substrates are illustrated in Figure 3. The substrate mobility and hydrophobicity increase as the PDMS coverage and thickness increase, from SiO_2 to LMW PDMS, to MMW PDMS, and to HMW PDMS.

Stability of PVOH Films on Various Substrates. Adsorptive spin coating of a 0.1 wt % PVOH$^{99\%H}$ solution on PDMS^{2k} and HMW PDMS substrates was evaluated in our earlier work.[18] In this study, we extended the study to two different PVOH degrees of hydrolysis (PVOH$^{99\%H}$ and PVOH$^{88\%H}$) and different PVOH concentrations (0.05 to 0.5 wt %) on all four types of substrates.

The AFM images of PVOH$^{99\%H,0.1wt\%}$ thin films spin-coated on SiO_2 as a function of spin rate are shown in the second column of Table 2. All films appear smooth; there is a slight decrease in the root-mean-square (rms) roughness values as the spin rate increases (Table S1). Similar observations were made with PVOH$^{88\%H,0.1wt\%}$ thin films spin-coated on SiO_2 (Table S1). To confirm their stability, the PVOH$^{99\%H}$ and PVOH$^{88\%H}$ films spin-coated at 6000 rpm were thermally annealed at 100 °C for up to 60 min. Bases on the AFM images (Table S2) and the PVOH film thickness values (Figure S1) before and after annealing, there is a negligible change upon annealing. We conclude that both PVOH$^{99\%H}$ and PVOH$^{88\%H}$ films on SiO_2 are stable systems where pinhole-free, thermodynamically stable films are formed at all thickness values.

PDMS^{340} was chosen to represent the LMW PDMS substrates. The AFM images of the PVOH$^{99\%H,0.1wt\%}$ thin films spin-coated on the substrate as a function of spin rate are shown in the third column of Table 2. Additional AFM images of PVOH$^{99\%H}$ and PVOH$^{88\%H}$ films prepared from different concentrations can be found in Tables S3 and S4. In general, surface coverage is sparse when PVOH films are thin, which occurs at low PVOH concentrations and high spin rates. On the other hand, surface coverage is continuous and pinhole-free

https://doi.org/10.1021/acs.langmuir.2c02206
Langmuir XXXX, XXX, XXX−XXX

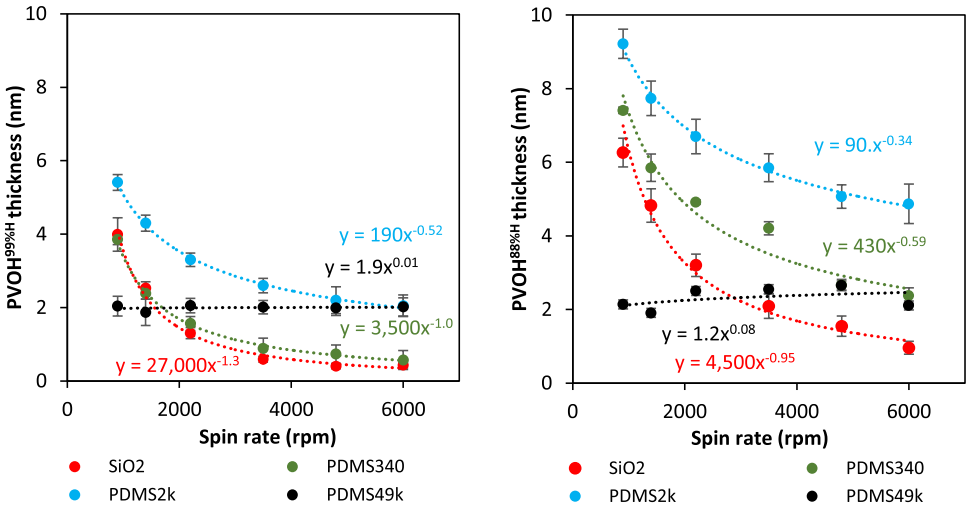

Figure 4. PVOH$^{99\%H,0.1wt\%}$ (left) and PVOH$^{88\%H,0.1wt\%}$ (right) film thickness as a function of spin rate (adsorption time = 1 min and spin time = 1 min) on SiO_2 (red curve), LMW PDMS^{340} (green curve), MMW PDMS^{2k} (blue curve), and HMW PDMS (black curve) substrates.

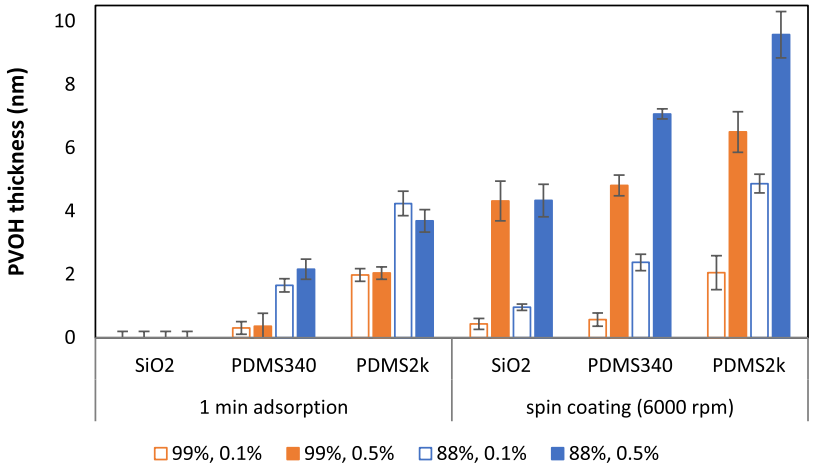

Figure 5. Comparison between 1 min static adsorption thickness and spin-coated thickness at 6000 rpm on SiO_2, PDMS^{340}, and PDMS^{2k} substrates using different PVOH solutions.

when PVOH films are thick, which occurs at high PVOH concentrations and low spin rates. Various types of dewetting patterns, including thermal nucleation and spinodal dewetting, are observed at intermediate thickness values, as shown in Figure S2.

PDMS^{2k} was chosen to represent the MMW PDMS substrates. The AFM images of the PVOH$^{99\%H,0.1wt\%}$ thin films spin-coated on the substrate as a function of spin rate are shown in the last column of Table 2. The morphological transition of the PVOH thin films from continuous to discontinuous as spin rate increases is similar to that on the PDMS^{340} substrate. The PVOH films on these two types of substrates show characteristics of metastable systems—thicker films obtained at lower spin rates are continuous, while thinner films obtained at higher spin rates exhibit dewetting patterns.

In one of our earlier reports, the spin dynamics of a 200 μL PVOH drop on PDMS^{2k} (MMW) and PDMS^{49k} (HMW) substrates were captured using a high-speed camera.[18] Macroscopic wetting was observed on the PDMS^{2k} substrate—after the exit of the excess solution, the rest of the drop remained pinned. This indicates that macroscopic wetting can still result in nanoscopic dewetting in a metastable system. The video captured by the high-speed camera also revealed macroscopic dewetting of the PVOH drop on the PDMS^{49k} substrate—after the initial exit of the excess solution, the rest of the drop receded and spun off in a stepwise fashion. The optical microscopy images of the PVOH thin films spin-coated on PDMS^{49k} exhibited extensive dewetting patterns at all spin rates.[18] The optical images of the adsorbed PVOH films on the HMW PDMS substrates also show micron-scale dewetting patterns.[33] The PVOH thin films on PDMS^{49k} (and other HMW PDMS) substrates have the characteristics of unstable systems.

Relationship between Film Stability and Thickness-Spin Rate Profile. The Meyerhofer model established a thickness-spin rate profile—the dependence of film thickness (h) on spin rate (ω) being $h = k\omega^{-1/2}$, where k is related to the initial solution concentration. One of the main objectives of this research is to discern whether the exponent n in $h = k\omega^{-n}$ depends on film stability.

The thickness-spin rate profiles using PVOH$^{99\%H,0.1wt\%}$ and PVOH$^{88\%H,0.1wt\%}$ on SiO_2, PDMS^{340}, PDMS,^{2k} and PDMS^{49k} are shown in Figure 4. The corresponding log–log plots are shown in Figure S3. It is worth noting that all of the thickness measurements were made away from the sample edges because the cast PVOH drops did not cover the entire samples, and the

https://doi.org/10.1021/acs.langmuir.2c02206
Langmuir XXXX, XXX, XXX−XXX

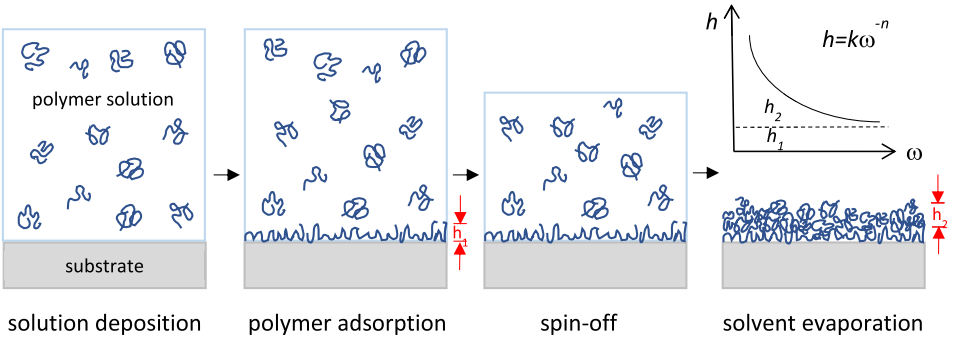

Figure 6. Proposed adsorption−deposition model partitioning the total polymer thickness into spontaneously adsorbed thickness (h_1) and spin-deposited thickness (h_2) using the adsorptive spin-coating method.

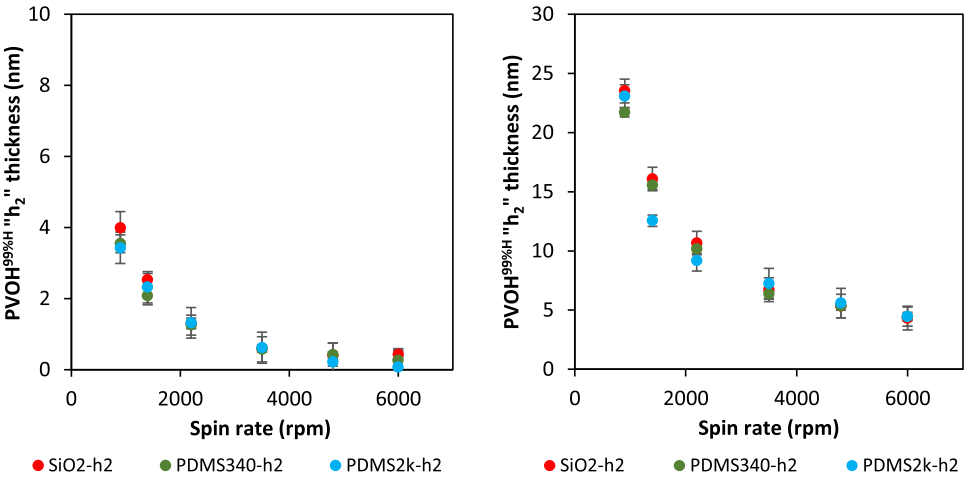

Figure 7. Spin-deposition thickness "h_2" on SiO_2, $PDMS^{340}$, and $PDMS^{2k}$ substrates as a function of spin rate using 0.1 wt % (left) and 0.5 wt % (right) $PVOH^{99\%H}$ solutions.

dried PVOH films often exhibit edge effects, such as coffee rings. Surprisingly, all eight curves are nonoverlapping and have different exponents. Both $PVOH^{99\%H,0.1wt\%}$ and $PVOH^{88\%H,0.1wt\%}$ curves on $PDMS^{49k}$ show n = ∼0, implying that film thickness is independent of spin rate in the unstable systems where "slip" takes place at the substrate−solution interface during spin. This phenomenon has been elucidated in one of our earlier reports.[18] Thus, we will focus our attention on the stable and metastable systems in this study. The following observations can be made. The $PVOH^{88\%H}$ films are significantly thicker than the $PVOH^{99\%H}$ counterparts. In the stable systems, the $PVOH^{99\%H,0.1\ wt\%}$ and $PVOH^{88\%H,0.1wt\%}$ curves on SiO_2 are steep, with n being 1.3 and 0.95, respectively. In the metastable systems, the curves have n ranging from 0.34 to 1. When 0.5 wt % PVOH solutions were used, all thickness profiles shifted upward, as shown in Figure S4.

Static Adsorption of PVOH. To rationalize the different thickness-spin rate profiles, static adsorption of PVOH on SiO_2, $PDMS^{340}$, and $PDMS^{2k}$ was carried out. The duration of the adsorption was kept at 1 min to mimic the adsorption step in the adsorptive spin-coating protocol.

The left half of Figure 5 depicts the adsorbed thickness from 0.1 and 0.5 wt % $PVOH^{99\%H}$ and $PVOH^{88\%H}$ solutions on the three substrates. Since hydrophobic interaction is the driving force for adsorption, the adsorbed thickness increases as substrate hydrophobicity increases, with negligible adsorption on the extremely hydrophilic SiO_2 and the largest adsorbed amount on the most hydrophobic $PDMS^{2k}$. Furthermore, the more hydrophobic $PVOH^{88\%H}$ results in thicker adsorbed films than $PVOH^{99\%H}$, which is consistent with the earlier reports.[29,32] It is also worth noting that PVOH concentration does not affect the spontaneously adsorbed amount under the conditions examined. The right half of Figure 5 depicts the spin-coated thickness obtained at 6000 rpm, which is the highest spin rate used to produce the thinnest films in this work. The spin-coated thickness scales with substrate and PVOH hydrophobicity as well as PVOH concentration. The thickness difference between spin coating and static adsorption is plotted in Figure S5. It is apparent that the spin-coated thickness at 6000 rpm is comparable to, albeit slightly larger than, the adsorbed thickness at the low polymer concentration of 0.1 wt %. On the other hand, the spin-coated thickness at 6000 rpm is significantly larger than the adsorbed thickness at the higher polymer concentration of 0.5 wt %.

Proposed Adsorption−Deposition Model to Rationalize Thickness-Spin Rate Profiles—h_1 and h_2. Based on Figure 5 and results from our earlier work,[18] a polymer thin film prepared by adsorptive spin coating consists of two components—a base layer (with thickness h_1) and a top layer (with thickness h_2). The former is spontaneously adsorbed at the solution−substrate interface during the adsorption step, and the latter is deposited during the spin process, as illustrated in Figure 6. The usage of "base" and "top" does not imply that a deposited polymer film has a stratified layer structure.

https://doi.org/10.1021/acs.langmuir.2c02206
Langmuir XXXX, XXX, XXX−XXX

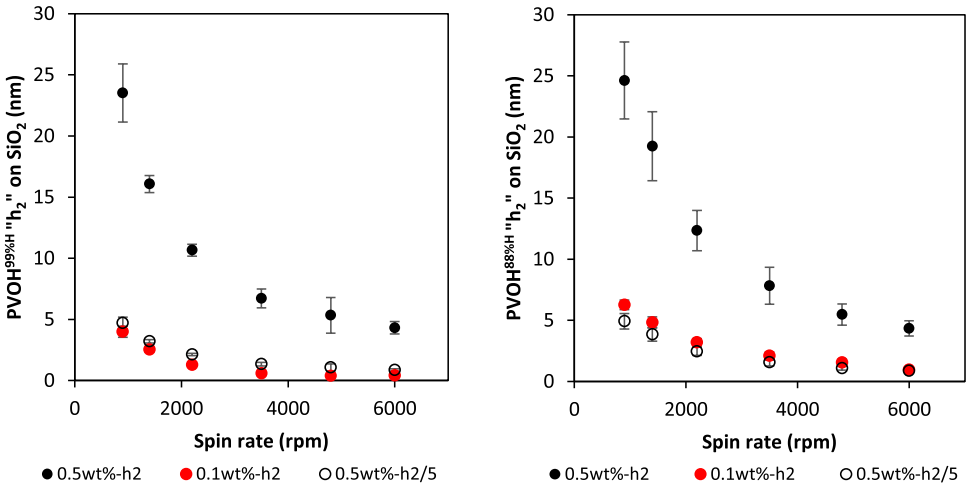

Figure 8. Spin-deposition thickness "h_2" as a function of spin rate and PVOH (left: 99%H and right: 88%H) concentration on SiO_2 substrate: filled red and black symbols represent h_2 thickness values using 0.1 and 0.5 wt % solutions, respectively; open black symbols represent 1/5 of h_2 thickness values from 0.5 wt % solutions.

Instead, they represent the sequence of two different events contributing to the overall film thickness, h.

The thickness of the base layer, h_1, depends on polymer−substrate interactions, which contributes to most of the thickness obtained at the highest spin rate examined, 6000 rpm. In metastable and stable systems, the thickness of the top layer, h_2, largely depends on solution concentration and spin rate. It contributes to most of the thickness obtained at the lowest spin rate examined, 900 rpm. To a first approximation, the exponent, n, should depend on the relative values of h_1 and h_2.

The exception is unstable systems, where extensive dewetting takes place, resulting in a negligible deposition during the spin process. The constant film thickness on $PDMS^{49k}$ (black series in Figure 4) thus corresponds to the spontaneously adsorbed amount, h_1. In the following sections, the effects of polymer−substrate interactions, polymer concentration, and polymer type in metastable and stable systems are analyzed in detail.

Effect of Polymer−Substrate Interactions on h_1. To test the validity of the proposed model, the 1 min adsorption thickness (h_1, Figure 5) was subtracted from the total thickness ($h_1 + h_2$, Figures 4 and S4) to obtain the spin-deposited thickness (h_2). Figure 7 depicts h_2 thickness of $PVOH^{99\%H}$ films as a function of spin rate on SiO_2, $PDMS^{340}$, and $PDMS^{2k}$ substrates. It is striking that the three curves corresponding to different substrates converge when the same $PVOH^{99\%H}$ concentration, 0.1 or 0.5 wt %, was used. The same convergence was observed for $PVOH^{88\%H}$ films (Figure S6). The incomplete film drying and "puddle" formation at the sample corners during spin coating contribute to the larger deviations at 900 and 1400 rpm. This validates the assumption that the spontaneously adsorbed thickness, h_1, is the only component in the total thickness that reflects polymer−substrate interactions.

Effect of Polymer Concentration on h_2. The h_2 thicknesses obtained from the 0.5 wt % solution are significantly larger than those from the 0.1 wt % solution (Figure 7). To quantify the effect of polymer concentration, the h_2 thicknesses corresponding to the two different concentrations are plotted as a function of spin rate on SiO_2 (Figure 8). The filled black and red symbols represent the h_2 thicknesses from the 0.5 and 0.1 wt % solutions, respectively. The third data series represented by the open black symbols was obtained after dividing the h_2 thicknesses from the 0.5 wt % series by 5, which is the ratio between the two concentrations. It is notable that the new and the 0.1 wt % data series converge on SiO_2 as well as on $PDMS^{340}$ (Figure S7) and $PDMS^{2k}$ (Figure S8). This factor of 5 difference was observed in all of the polymer series, independent of the substrate. Considering the human errors in multistep sample preparation, instrument-related measurement errors, and the uneven mass distributions across dewetted thin films, the superposition of the different curves is remarkable. These results suggest that h_2 thickness is proportional to polymer concentration and is independent of polymer−substrate interactions.

Effect of Polymer−Polymer Interactions. In this study, PVOH polymers of two different degrees of hydrolysis, $PVOH^{88\%H}$ and $PVOH^{99\%H}$, were examined. As shown in Figure S9, the $PVOH^{88\%H,0.1wt\%}$ films have significantly larger h_2 thicknesses than $PVOH^{99\%H,0.1wt\%}$ films across all spin rates. The thickness difference between the two types of polymers decreases from ∼2 to ∼0.5 nm as the spin rate increases, independent of substrate type. One possible explanation is that the adsorption step results in a strongly adsorbed inner layer (h_1) as well as a weakly adsorbed outer layer. The latter is mostly removed during the rinsing process using the static adsorption method, while it is partially retained using the spin-coating method. The strong shear force at a high spin rate can remove more of the weakly bound layer than at a lower spin rate. The adsorption of $PVOH^{88\%H}$ most likely results in a more pronounced weakly bound outer layer due to the stronger hydrophobic interactions between polymer chains.

All of the experimental data presented thus far are consistent with the proposed adsorption−deposition model. It is tempting to propose a new universal relationship between spin-coated thickness (h) and spin rate (ω) that includes the effects of adsorption. In such a relationship, the adsorbed amount (h_1) is dependent on polymer−substrate interactions and should be removed. The deposited amount (h_2) is proportional to polymer concentration and is required to be accounted for. However, the dependence of adsorption on polymer type and the presence of a weakly adsorbed layer in

https://doi.org/10.1021/acs.langmuir.2c02206
Langmuir XXXX, XXX, XXX−XXX

some systems render the relationship polymer-specific (and spin rate-dependent). Since PVOH does not spontaneously adsorb to SiO_2 ($h_1 = 0$), the fitted equations on SiO_2 shown in Figure 4 can be used: h_2 (in nm) = 2.7 × 104 $\omega^{-1.3}$ for $PVOH^{99\%H}$ and h_2 (in nm) = 4.5 × 103 $\omega^{-0.95}$ for $PVOH^{88\%H}$, with the proportionality constants corresponding to 0.1 wt % polymer concentration.

Most of the previous studies on spin coating used the highly energetic silicon wafer as the substrate, which most polymers, such as the two PVOH polymers in this study, do not adsorb to. However, a wide range of substrates with different chemical and physical characteristics are presented in real-life applications. Spontaneous polymer adsorption driven by hydrophobic interactions, electrostatic attractions, hydrogen bonding, and/or dipole−dipole interactions take place in many polymer−substrate systems. It is crucial to take into account such interactions when predicting film thickness. The most unexpected outcome of this study is that the Meyerhofer exponent of 1/2 was not observed for the PVOH films on SiO_2, where polymer adsorption is absent. Instead, much larger exponents of 1.3 for $PVOH^{99\%H}$ and 0.95 for $PVOH^{88\%H}$ were obtained. The investigation of the significant deviations of these hydrophilic polymer systems from the Meyerhofer exponent is currently ongoing.

CONCLUSIONS

Adsorptive spin coating of 88% and 99% hydrolyzed PVOH was carried out on four SiO_2/PDMS composite substrates with varying energetics and mobility. The stability of the PVOH thin films decreased as substrate hydrophobicity and mobility increased—stable on SiO_2, metastable on LMW and MMW PDMS, and unstable on HMW PDMS. To account for the large discrepancies between our experimental data and the well-established Meyerhofer model, $h \propto \omega^{-1/2}$, a new model to decouple the total spin-coated thickness into two components—the adsorbed thickness h_1 and the spin-deposited thickness h_2—was proposed. The former largely depends on polymer−substrate interactions, and the latter is mostly dependent on polymer concentration and spin rate. Our model is successful at fitting the experimental data in the polymer−substrate systems of different film stabilities. In the unstable systems, the film thickness is predominantly h_1 and is independent of spin rate because of slip at the solution−substrate interface. In the stable and metastable systems, one master curve correlating h_2 and ω was constructed on the different substrates for each of the PVOH polymers.

ASSOCIATED CONTENT

Supporting Information

The Supporting Information is available free of charge at https://pubs.acs.org/doi/10.1021/acs.langmuir.2c02206.

Additional AFM images and thickness data of PVOH thin films on different substrates (PDF)

AUTHOR INFORMATION

Corresponding Author

Wei Chen − *Chemistry Department, Carr Laboratory, Mount Holyoke College, South Hadley, Massachusetts 01075, United States;* orcid.org/0000-0002-6970-3455; Email: weichen@mtholyoke.edu

Authors

Yuxin Jiang − *Chemistry Department, Carr Laboratory, Mount Holyoke College, South Hadley, Massachusetts 01075, United States*

Margaret Minett − *Chemistry Department, Carr Laboratory, Mount Holyoke College, South Hadley, Massachusetts 01075, United States*

Elizabeth Hazen − *Chemistry Department, Carr Laboratory, Mount Holyoke College, South Hadley, Massachusetts 01075, United States*

Wenyun Wang − *Chemistry Department, Carr Laboratory, Mount Holyoke College, South Hadley, Massachusetts 01075, United States*

Carolina Alvarez − *Chemistry Department, Carr Laboratory, Mount Holyoke College, South Hadley, Massachusetts 01075, United States*

Julia Griffin − *Chemistry Department, Carr Laboratory, Mount Holyoke College, South Hadley, Massachusetts 01075, United States*

Nancy Jiang − *Chemistry Department, Carr Laboratory, Mount Holyoke College, South Hadley, Massachusetts 01075, United States*

Complete contact information is available at: https://pubs.acs.org/10.1021/acs.langmuir.2c02206

Notes

The authors declare no competing financial interest.

ACKNOWLEDGMENTS

Financial support was provided by the National Science Foundation (DMR-1807186) and Mount Holyoke College.

REFERENCES

(1) Vrij, A. Possible Mechanism for the Spontaneous Rupture of Thin, Free Liquid Films. *Discuss. Faraday Soc.* **1966**, *42*, 23−33.

(2) Reiter, G. Dewetting of Thin Polymer Films. *Phys. Rev. Lett.* **1992**, *68*, 75−78.

(3) Reiter, G. Unstable Thin Polymer Films: Rupture and Dewetting Processes. *Langmuir* **1993**, *9*, 1344−1351.

(4) Sharma, A. Relationship of Thin Film Stability and Morphology to Macroscopic Parameters of Wetting in the Apolar and Polar Systems. *Langmuir* **1993**, *9*, 861−869.

(5) Stange, T. G.; Evans, D. F.; Hendrickson, W. A. Nucleation and Growth of Defects Leading to Dewetting of Thin Polymer Films. *Langmuir* **1997**, *13*, 4459−4465.

(6) Thiele, U.; Mertig, M.; Pompe, W. Dewetting of an Evaporating Thin Liquid Film: Heterogeneous Nucleation and Surface Instability. *Phys. Rev. Lett.* **1998**, *80*, 2869−2872.

(7) Xie, R.; Karim, A.; Douglas, J. F.; Han, C. C.; Weiss, R. A. Spinodal Dewetting of Thin Polymer Films. *Phys. Rev. Lett.* **1998**, *81*, 1251−1254.

(8) Seemann, R.; Herminghaus, S.; Jacobs, K. Dewetting Patterns and Molecular Forces: A Reconciliation. *Phys. Rev. Lett.* **2001**, *86*, 5534−5537.

(9) Ramanathan, M.; Darling, S. B. Mesoscale Morphologies in Polymer Thin Films. *Prog. Polym. Sci.* **2011**, *36*, 793−812.

(10) Xue, L.; Han, Y. Pattern Formation by Dewetting of Polymer Thin Film. *Prog. Polym. Sci.* **2011**, *36*, 269−293.

(11) Gentili, D.; Foschi, G.; Valle, F.; Cavallini, M.; Biscarini, F. Applications of Dewetting in Micro and Nanotechnology. *Chem. Soc. Rev.* **2012**, *41*, 4430−4443.

(12) Mukherjee, R.; Sharma, A. Instability, Self-Organization and Pattern Formation in Thin Soft Films. *Soft Matter* **2015**, *11*, 8717−8740.

(13) Bathawab, F.; Bennett, M.; Cantini, M.; Reboud, J.; Dalby, M. J.; Salmerón-Sánchez, M. Lateral Chain Length in Polyalkyl Acrylates Determines the Mobility of Fibronectin at the Cell/Material Interface. *Langmuir* **2016**, *32*, 800−809.
(14) Bieniek, M. K.; Llopis-Hernandez, V.; Douglas, K.; Salmerón-Sánchez, M.; Lorenz, C. D. Minor Chemistry Changes Alter Surface Hydration to Control Fibronectin Adsorption and Assembly into Nanofibrils. *Adv. Theory Simul.* **2019**, *2*, No. 1900169.
(15) Zhang, Y.; Ng, S.-W.; Lu, X.; Zheng, Z. Solution-Processed Transparent Electrodes for Emerging Thin-Film Solar Cells. *Chem. Rev.* **2020**, *120*, 2049−2122.
(16) Zhou, L.; Jiang, Y. Recent Progress in Dielectric Nanocomposites. *Mater. Sci. Technol.* **2020**, *36*, 1−16.
(17) Bornside, D. E.; Macosko, C. W.; Scriven, L. E. On the Modeling of Spin Coating. *J. Imaging Technol.* **1987**, *13*, 122−130.
(18) Qi, Y.; Nguyen, H.; Lim, K. S. E.; Wang, W.; Chen, W. Adsorptive Spin Coating to Study Thin-Film Stability in Both Wetting and Nonwetting Regimes. *Langmuir* **2019**, *35*, 6922−6928.
(19) Le, M. L.; Zhou, Y.; Byun, J.; Kolozsvari, K.; Xu, S.; Chen, W. Using A Spin-Coater to Capture Adhesive Species During Polydopamine Thin-Film Fabrication. *Langmuir* **2019**, *35*, 12722−12730.
(20) Emslie, A. G.; Bonner, F. T.; Peck, L. G. Flow of a Viscous Liquid on a Rotating Disk. *J. Appl. Phys.* **1958**, *29*, 858−862.
(21) Meyerhofer, D. Characteristics of Resist Films Produced by Spinning. *J. Appl. Phys.* **1978**, *49*, 3993−3997.
(22) Extrand, C. W. Continuity of Very Thin Polymer Films. *Langmuir* **1993**, *9*, 475−480.
(23) Extrand, C. W. Spin Coating of Very Thin Polymer Films. *Polym. Eng. Sci.* **1994**, *34*, 390−394.
(24) Danglad-Flores, J.; Eickelmann, S.; Riegler, H. Deposition of Polymer Films by Spin Casting: A Quantitative Analysis. *Chem. Eng. Sci.* **2018**, *179*, 257−264.
(25) Lawrence, C. J. The Mechanics of Spin Coating of Polymer Films. *Phys. Fluids* **1988**, *31*, 2786−2795.
(26) Mao, D.; Lv, G.; Gao, G.; Fan, B. Fabrication of Polyimide Films with Imaging Quality Using A Spin-Coating Method for Potential Optical Applications. *J. Polym. Eng.* **2019**, *39*, 917−925.
(27) Coupe, B.; Chen, W. A New Approach to Surface Functionalization of Fluoropolymers. *Macromolecules* **2001**, *34*, 1533−1535.
(28) Kozlov, M.; Quarmyne, M.; Chen, W.; McCarthy, T. J. Adsorption of Poly(vinyl alcohol) onto Hydrophobic Substrates. A General Approach for Hydrophilizing and Chemically Activating Surfaces. *Macromolecules* **2003**, *36*, 6054−6059.
(29) Kozlov, M.; McCarthy, T. J. Adsorption of Poly(vinyl alcohol) From Water to a Hydrophobic Surface: Effects of Molecular Weight, Degree of Hydrolysis, Salt, and Temperature. *Langmuir* **2004**, *20*, 9170−9176.
(30) Barrett, D. A.; Hartshorne, M. S.; Hussain, M. A.; Shaw, P. N.; Davies, M. C. Resistance to Nonspecific Protein Adsorption by Poly(vinyl alcohol) Thin Films Adsorbed to a Poly(styrene) Support Matrix Studied Using Surface Plasmon Resonance. *Anal. Chem.* **2001**, *73*, 5232−5239.
(31) Serizawa, T.; Hashiguchi, S.; Akashi, M. Stepwise Assembly of Ultrathin Poly(vinyl alcohol) Films on a Gold Substrate by Repetitive Adsorption/Drying Processes. *Langmuir* **1999**, *15*, 5363−5368.
(32) Karki, A.; Nguyen, L.; Sharma, B.; Yan, Y.; Chen, W. Unusual Morphologies of Poly(vinyl alcohol) Thin Films Adsorbed on Poly(dimethylsiloxane) Substrates. *Langmuir* **2016**, *32*, 3191−3198.
(33) Krumpfer, J. W.; McCarthy, T. J. Rediscovering Silicones: "Unreactive" Silicones React with Inorganic Surfaces. *Langmuir* **2011**, *27*, 11514−11519.
(34) Cassie, A. B. D. Contact Angles. *Discuss. Faraday Soc.* **1948**, *3*, 11−16.
(35) Israelachvili, J. N.; Gee, M. L. Contact Angles on Chemically Heterogeneous. *Surfaces* **2015**, *5*, 288−289.

https://doi.org/10.1021/acs.langmuir.2c02206
Langmuir XXXX, XXX, XXX−XXX